MCB
Journals.ASM.org

ATF1 Modulates the Heat Shock Response by Regulating the Stress-Inducible Heat Shock Factor 1 Transcription Complex

Ryosuke Takii,[a] Mitsuaki Fujimoto,[a] Ke Tan,[a] Eiichi Takaki,[a] Naoki Hayashida,[a] Ryuichiro Nakato,[b] Katsuhiko Shirahige,[b] Akira Nakai[a]

Department of Biochemistry and Molecular Biology, Yamaguchi University School of Medicine, Minami-Kogushi, Ube, Japan[a]; Research Center for Epigenetic Disease, Institute of Molecular and Cellular Biosciences, The University of Tokyo, Tokyo, Japan[b]

The heat shock response is an evolutionally conserved adaptive response to high temperatures that controls proteostasis capacity and is regulated mainly by an ancient heat shock factor (HSF). However, the regulation of target genes by the stress-inducible HSF1 transcription complex has not yet been examined in detail in mammalian cells. In the present study, we demonstrated that HSF1 interacted with members of the ATF1/CREB family involved in metabolic homeostasis and recruited them on the *HSP70* promoter in response to heat shock. The HSF1 transcription complex, including the chromatin-remodeling factor BRG1 and lysine acetyltransferases p300 and CREB-binding protein (CBP), was formed in a manner that was dependent on the phosphorylation of ATF1. ATF1-BRG1 promoted the establishment of an active chromatin state and *HSP70* expression during heat shock, whereas ATF1-p300/CBP accelerated the shutdown of HSF1 DNA-binding activity during recovery from acute stress, possibly through the acetylation of HSF1. Furthermore, ATF1 markedly affected the resistance to heat shock. These results revealed the unanticipated complexity of the primitive heat shock response mechanism, which is connected to metabolic adaptation.

All living cells maintain a balance among the synthesis, folding, and clearance of individual proteins in order to maintain the proper conformations and physiological concentrations of proteins, and this is referred to as protein homeostasis or proteostasis (1). To survive temperature elevations, which cause protein unfolding and misfolding, cells induce the expression of a small number of highly conserved heat shock proteins (HSPs or chaperones) and hundreds of non-HSP proteins involved in diverse functions, including protein degradation (2, 3). Thus, this universal adaptive response, which is known as the heat shock response, controls the proteostasis capacity or buffering capacity against protein misfolding in a cell (4) and is regulated mainly at the level of transcription by the ancient transcription factor σ32 in *Escherichia coli* (5) or heat shock factor (HSF) in eukaryotes (6, 7).

In contrast to the *E. coli* genome, which is compressed into a small space through supercoiling (8), eukaryotic genomes are packaged into nucleosomes, which are composed of DNA wrapped around the histone octamer and occlude DNA from interacting with most DNA-binding proteins (9). To induce transcription during heat shock, HSF binds to regulatory elements and recruits coactivators, including chromatin-modifying enzymes and nucleosome-remodeling complexes that move or displace histones at the promoter and gene body (10). Metazoan HSF remains mostly as an inactive monomer in unstressed cells and is converted to an active trimer that binds to the heat shock response element (HSE) during heat shock (11). In *Drosophila*, the GAGA factor restricts the nucleosome occupancy of the *HSP70* promoter, thereby allowing the establishment of paused RNA polymerase II (Pol II) in unstressed cells (12). In response to heat shock, the increased levels of DNA-bound HSF recruit the elongation factors, such as P-TEFb and Spt6, and histone-modifying enzymes, such as CREB-binding protein (CBP) and Tip60, on the *HSP70* promoter, and this is accompanied by the activation and spread of poly(ADP-ribose) polymerase (13, 14, 15). This activator-dependent recruitment of coactivators was previously shown to be followed by the rapid loss of nucleosomes, release of stalled Pol II, and induction of gene expression (12, 16).

HSF1 is a master regulator of HSP expression in mammals, whereas all HSF family members (HSF1 to -4) are involved in the regulation of proteostasis capacity through HSP and non-HSP pathways (17, 18). Even under normal physiological conditions, a small amount of the HSF1 trimer binds to nucleosomal DNA in complex with replication protein A and a histone chaperone and regulates basal gene expression and proteostasis capacity (19). Therefore, a deficiency in HSF1 reduces proteostasis capacity in mammalian cells and accelerates progression in mouse models of protein misfolding diseases (20), such as that of worm HSF1 (4). Although HSF1 has been shown to robustly recruit the SWI/SNF chromatin-remodeling complex including BRG1 and the lysine acetyltransferase p300 on the *HSP70* promoter during heat shock (21, 22), components of the stress-inducible HSF1 transcription complex or the regulation of this complex formation have yet to be examined in detail in mammalian cells.

To elucidate the HSF1 transcription complex more clearly, we previously identified many proteins interacting with human HSF1 (hHSF1) and suggested that hHSF1 may interact with the ATF1/CREB family members (ATF1, CREB, and CREM) (19) involved in homeostasis and metabolic adaptation (23). In the present study, we demonstrated that all ATF1/CREB family members play roles in the induction of *HSP70* expression during heat shock or its

Received 2 June 2014 **Returned for modification** 7 August 2014
Accepted 6 October 2014

Accepted manuscript posted online 13 October 2014

Citation Takii R, Fujimoto M, Tan K, Takaki E, Hayashida N, Nakato R, Shirahige K, Nakai A. 2015. ATF1 modulates the heat shock response by regulating the stress-inducible heat shock factor 1 transcription complex. Mol Cell Biol 35:11–25. doi:10.1128/MCB.00754-14.

Address correspondence to Akira Nakai, anakai@yamaguchi-u.ac.jp.

Supplemental material for this article may be found at http://dx.doi.org/10.1128/MCB.00754-14.

doi:10.1128/MCB.00754-14

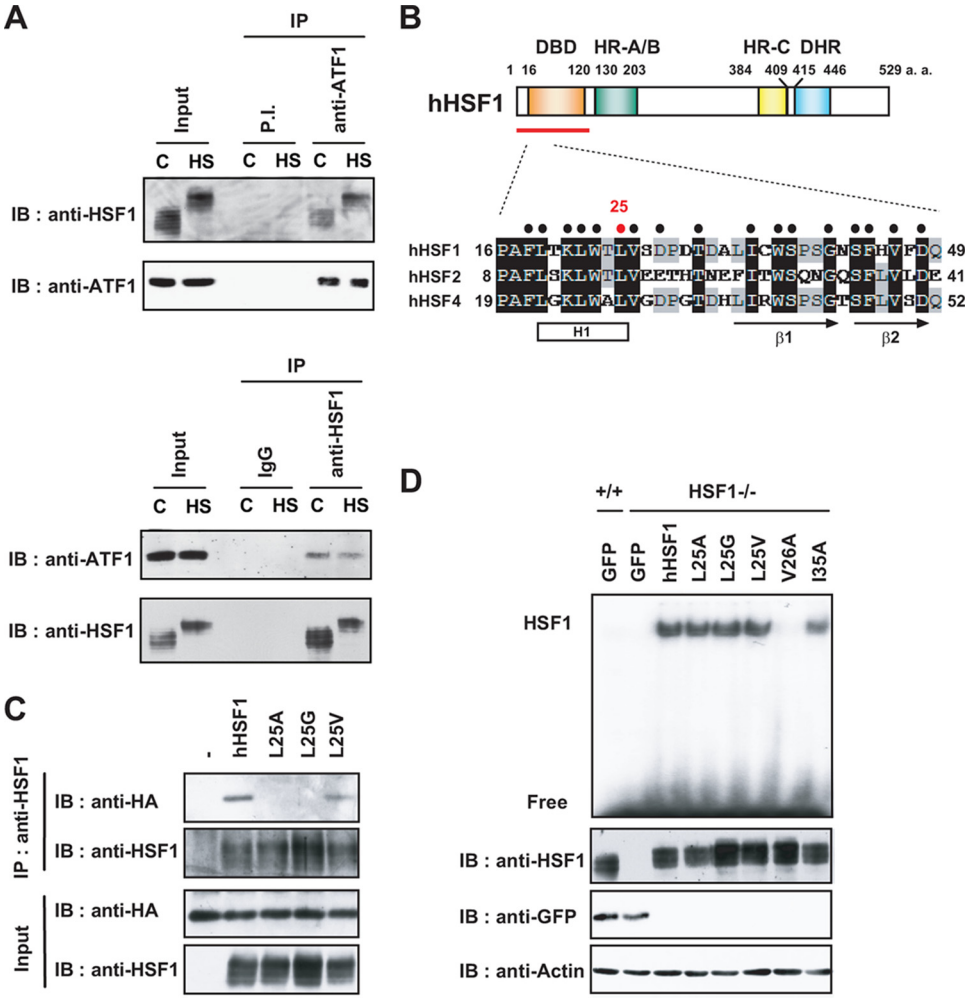

FIG 1 ATF1 bound to the DNA-binding domain of HSF1. (A) Interaction between HSF1 and ATF1. Extracts were prepared from control MEF cells at 37°C (lanes C), and cells were heat shocked at 42°C for 30 min (lanes HS). Complexes coimmunoprecipitated (IP) with preimmune (P.I.) serum or antiserum for ATF1 were immunoblotted (IB) with HSF1 or ATF1 antibody (top). Complexes coimmunoprecipitated with IgG or antibody to HSF1 were also blotted with ATF1 or HSF1 antibody (bottom). (B) Schematic representation of the ATF1-interacting region (red bar) in hHSF1 (top). DBD, DNA-binding domain; HR, hydrophobic heptad repeat; DHR, downstream of HR-C. An alignment of the amino acid (a.a.) sequences of N4 regions in the DBD of hHSFs is shown at the bottom. Seventeen residues in hHSF1 were conserved in both hHSF2 and hHSF4 (dots). (C) HSF1-L25 mutants did not interact with ATF1. HSF1-null MEF cells were infected with adenovirus expressing HA-mATF1, wild-type hHSF1, or mutant hHSF1 proteins. Complexes coimmunoprecipitated with HSF1 by HSF1 antibody were immunoblotted with HA or HSF1 antibody. (D) DNA-binding activities of HSF1-L25 mutants. Wild-type (+/+) and HSF1-null (−/−) MEF cells were infected with adenovirus expressing green fluorescent protein (GFP), wild-type hHSF1, or mutant hHSF1 proteins. Whole-cell extracts from cells under unstressed conditions were prepared and subjected to EMSA (top), and Western blotting (bottom) was performed.

shutdown during recovery in mammalian cells. We examined the HSF1-ATF1 complex in detail and revealed that ATF1 regulates the stress-inducible HSF1 transcription complex including the coactivators BRG1 and p300/CBP in a manner that is dependent on the phosphorylation of ATF1. These components in the complex act differently on the chromatin structure and HSF1 DNA-binding activity. Furthermore, formation of the HSF1-ATF1 complex markedly influences resistance to heat shock.

MATERIALS AND METHODS

Plasmids. Adenovirus vectors expressing short hairpin RNAs (shRNAs) against mouse HSF1, ATF1, CREB, CREM, BRG1, p300, and CBP were generated as described previously (24), with the primers listed in Table S1 in the supplemental material. cDNAs for hemagglutinin (HA)-tagged mouse ATF1, CREB, and CREM were created by reverse transcriptase PCR (RT-PCR) with total RNA isolated from mouse embryo fibroblast (MEF) cells and inserted into pcDNA4/HisMax A (Life Technologies, Japan) at the EcoRI/XhoI (pcDNA4-HA-mATF1) and BamHI/EcoRI (pcDNA4-HA-mCREB and pcDNA4-HA-mCREM) sites. To generate the adenovirus expression vectors pAd-HA-mATF1, pAd-HA-mCREB, and pAd-HA-mCREM, the KpnI/XhoI fragment of each expression plasmid was inserted into a pShuttle-CMV vector (Stratagene). The expression vectors for HA-mATF1 having deletion and point mutations were generated by PCR with mutated internal primers as described previously (24), and sequences were verified with a model 3500 genetic analyzer (Applied Biosystems).

Cell cultures and RNA interference. Immortalized wild-type ($HSF1^{+/+}$; stock no. 10) and HSF1-null (−/−; stock no. 4) MEF cells (20) were maintained at 37°C in 5% CO_2 in Dulbecco's modified Eagle's medium containing 10% fetal bovine serum. MEF cells (stock no. 10) maintained at 37°C were infected with an adenovirus expressing each shRNA (1×10^8 PFU/ml) for 2 h and maintained with normal medium for 70 h.

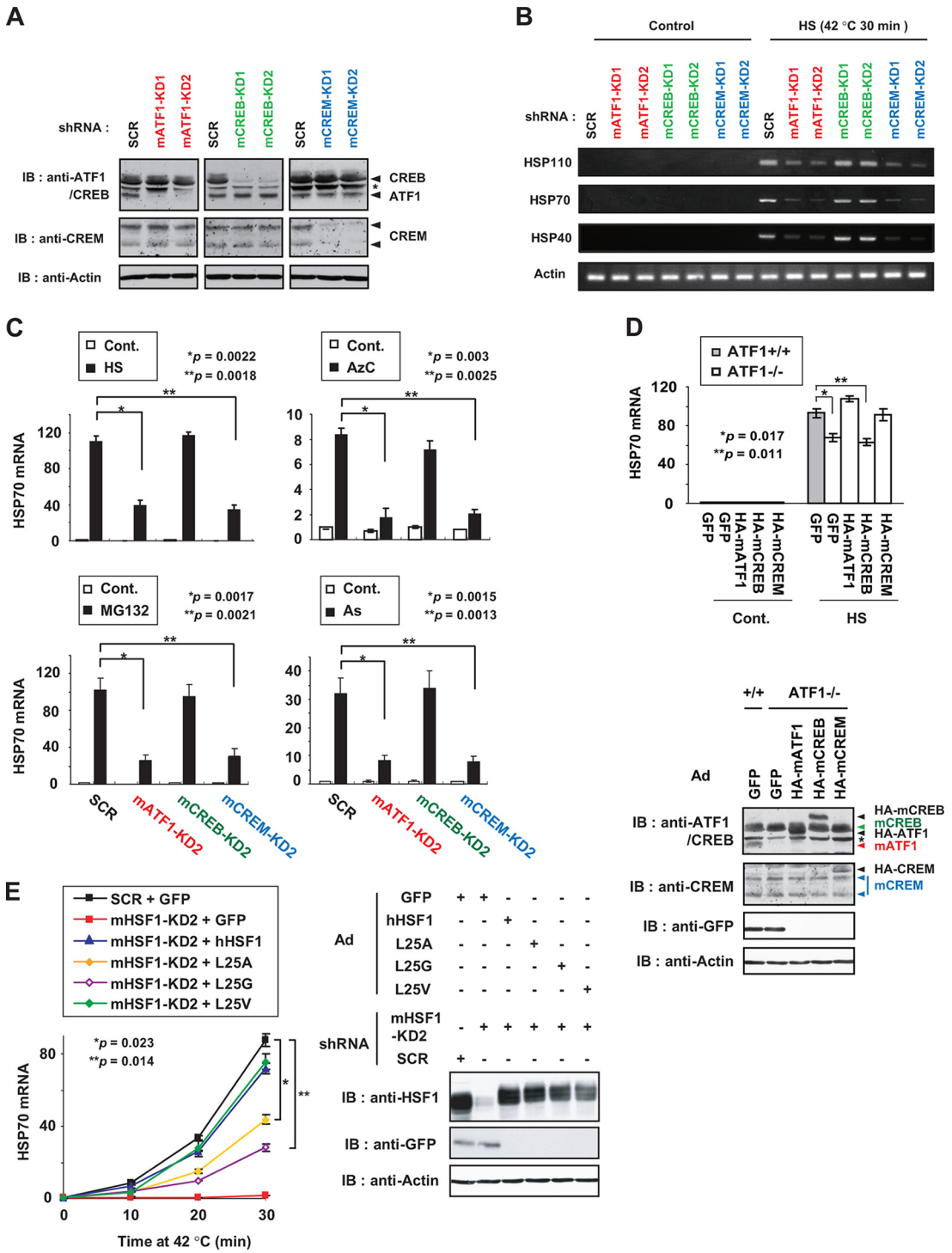

FIG 2 The HSF1-ATF1 complex promoted *HSP70* expression during heat shock. (A) Knockdown of mouse ATF1, CREB, and CREM. Immortalized MEF cells (stock no. 10) were infected for 72 h with adenovirus expressing shRNA against mATF1 (KD1, KD2), CREB (KD1, KD2), or CREM (KD1, KD2) or scrambled RNA (SCR). Cell extracts were prepared in NP-40 lysis buffer, and aliquots (120 μg) were subjected to Western immunoblotting (IB) with rabbit antibody to ATF1/CREB or CREM or mouse antibody to β-actin. Arrowheads indicate the positions of the proteins. The asterisk indicates nonspecific bands. (B) Knockdown of ATF1 and CREM reduced the mRNA expression of HSPs during heat shock. MEF cells that were infected with the adenovirus as described in panel A were treated without (Control) or with heat shock at 42°C for 30 min. The mRNA levels of HSPs, including HSP110, HSP70, and HSP40, and those of β-actin were determined by RT-PCR. (C) Expression of *HSP70* mRNA after the knockdown of ATF1/CREB members. ATF1, CREB, or CREM was knocked down in MEF cells and heat shocked at 42°C for 30 min (HS), MG132 for 3 h, AzC for 3 h, or As for 6 h. *HSP70* mRNA levels were determined by RT-PCR and quantified. *HSP70* mRNA levels relative to those in control Ad-sh-SCR-infected cells are shown ($n = 3$). (D) Overexpression of ATF1 or CREM rescued the expression of *HSP70* mRNA during heat shock in ATF1-null cells. GFP, HA-mATF1, HA-mCREB, or HA-mCREM was overexpressed in immortalized ATF1-null MEF cells. *HSP70* mRNA levels during heat shock at 42°C for 30 min (HS) were quantified by RT-qPCR. *HSP70* mRNA levels relative to those in control Ad-GFP-infected cells are shown (top). Error bars show the mean ± SD ($n = 3$). Significance (*P* value) was determined with an unpaired *t* test. Western blotting was performed with each specific antibody (bottom). Arrowheads indicate the positions of endogenous ATF1/CREB members and ectopically expressed proteins. (E) Expression of *HSP70* mRNA during heat shock in the presence of mutant HSF1 proteins. Endogenous HSF1 was replaced with each mutant hHSF1 protein or GFP in MEF cells. *HSP70* mRNA levels during heat shock at 42°C for the times indicated were quantified by RT-qPCR (left). *HSP70* mRNA levels are shown ($n = 3$). Western blotting (right) was performed.

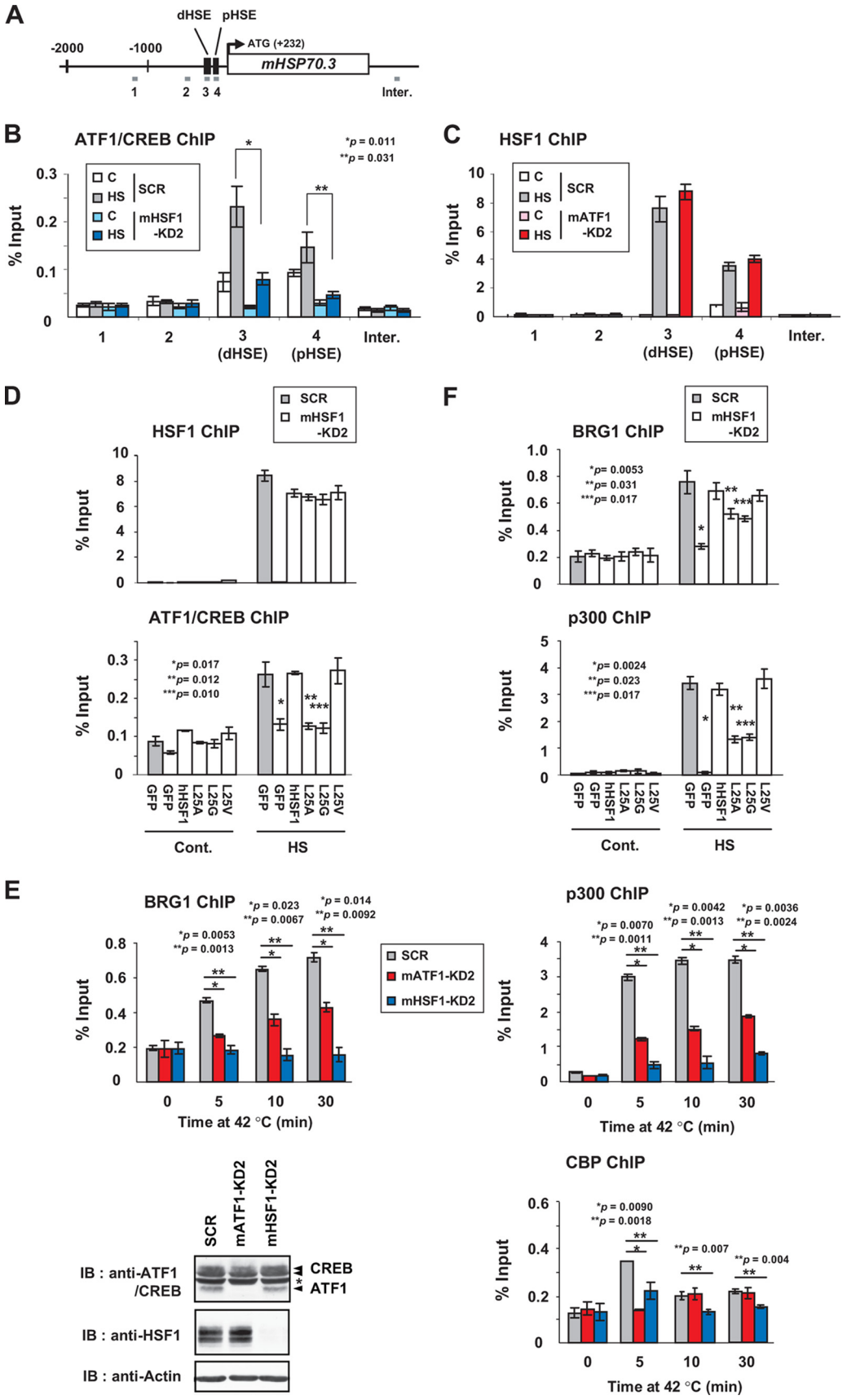
A
dHSE
pHSE
-2000
-1000
ATG (+232)
mHSP70.3
1
2
3
4
Inter.
B
ATF1/CREB ChIP
*p = 0.011
**p = 0.031
C
HS
SCR
mHSF1
-KD2
mATF1
% Input
(dHSE)
(pHSE)
C
HSF1 ChIP
D
HSF1 ChIP
ATF1/CREB ChIP
*p= 0.017
**p= 0.012
***p= 0.010
GFP
hHSF1
L25A
L25G
L25V
Cont.
HS
F
BRG1 ChIP
*p= 0.0053
**p= 0.031
***p= 0.017
p300 ChIP
*p= 0.0024
**p= 0.023
***p= 0.017
E
BRG1 ChIP
*p = 0.023
**p = 0.0067
*p = 0.014
**p = 0.0092
*p = 0.0053
**p = 0.0013
mATF1-KD2
mHSF1-KD2
Time at 42 °C (min)
p300 ChIP
*p = 0.0042
**p = 0.0013
*p = 0.0036
**p = 0.0024
*p = 0.0070
**p = 0.0011
IB : anti-ATF1
/CREB
CREB
ATF1
IB : anti-HSF1
IB : anti-Actin
CBP ChIP
*p = 0.0090
**p = 0.0018
**p = 0.007
**p = 0.004

Total RNA was extracted, and mRNA levels were estimated. Cell extracts were simultaneously prepared in NP-40 lysis buffer, and the knockdown of gene products was confirmed by Western blotting (19) with antibodies to HSF1 (anti-mHSF1j) (ABE1044; Merck Millipore), ATF1/CREB (sc-186; Santa Cruz), CREM (sc-440; Santa Cruz), p300 (sc-585; Santa Cruz), CBP (sc-369; Santa Cruz), BRG1 (07-478; Millipore), and phosphorylated ATF1-Ser63/CREB-Ser133 (no. 9198; Cell Signaling). To knock down the expression of endogenous HSF1 and overexpress mutant HSF1 proteins in MEF cells, the cells were infected with Ad-sh-mHSF1-KD2 (1×10^8 PFU/ml) for 2 h and maintained in normal medium for 22 h. They were then infected with an adenovirus expressing a mutant hHSF1 protein (1×10^7 to 5×10^7 PFU/ml) for 2 h and maintained with normal medium for a further 46 h. The replacement of endogenous ATF1 with its mutant was performed similarly.

Assessment of mRNA. Total RNA was isolated from cells with TRIzol (Invitrogen), and first-strand cDNA was synthesized with avian myeloblastosis virus RT and oligo$(dT)_{20}$ according to the manufacturer's instructions (Invitrogen). RT-PCR was performed, and the amplified DNA was stained with ethidium bromide. Signals were estimated by using the NIH Image program (25). Real-time quantitative PCR (qPCR) was performed with StepOnePlus (Applied Biosystems) with the Power SYBR green PCR master mix (Applied Biosystems) as described previously (19). The primers used for RT-qPCRs are listed in Table S2 in the supplemental material. The relative quantities of mRNAs were normalized against β-actin mRNA levels. All reactions were performed in triplicate with samples derived from three experiments.

Coimmunoprecipitation. MEF cells were lysed with NP-40 lysis buffer containing 1.0% Nonidet P-40, 150 mM NaCl, 50 mM Tris-HCl (pH 8.0), 1 μg/ml leupeptin, 1 μg/ml pepstatin, and 1 mM phenylmethylsulfonyl fluoride. After centrifugation, the supernatant containing 10 mg of proteins was incubated with 5 μl of the rabbit polyclonal antibody to ATF1 (anti-mATF1-1; see below) at 4°C for 16 h and mixed with 40 μl of protein A-Sepharose beads (GE Healthcare) by rotation at 4°C for 1 h. The complexes were washed five times with NP-40 lysis buffer and subjected to Western blotting with rat monoclonal IgG for HSF1 (ab61382; Abcam) or mouse monoclonal IgA for ATF1 (sc-243; Santa Cruz). Alternatively, the cell extract was incubated with 5 μg of rat monoclonal IgG for HSF1 (ab186359; Abcam) at 4°C for 16 h and mixed with 40 μl of protein G-Sepharose beads (GE Healthcare) by rotation at 4°C for 1 h. The complexes were washed and then subjected to Western blotting with the same HSF1 antibody or rabbit polyclonal antibody to ATF1 (anti-mATF1-1).

To perform coimmunoprecipitation with recombinant proteins, HEK293 cells transfected with an expression vector for HA-tagged wild-type, deletion-containing, or point-mutated mATF1 or with an expression vector for HA-mCREB or HA-mCREM were lysed with NP-40 lysis buffer. After centrifugation, the supernatant (500 μl) was incubated with 2 μl of the rabbit polyclonal antibody to HSF1 (αmHSF1j) (ABE1044; Merck Millipore) or 2 μg of the rat monoclonal antibody to HA (3F10; Roche) at 4°C for 1 h and mixed with 20 μl of protein A- or protein G-Sepharose beads (GE Healthcare) by rotation at 4°C for 1 h. These complexes were washed with NP-40 lysis buffer and then subjected to Western blotting with the rabbit antibody to HSF1 (αmHSF1j) or mouse IgG to HA. Alternatively, $HSF1^{-/-}$ MEF cells were coinfected with adenovirus expressing wild-type or point-mutated hHSF1 and adenovirus expressing HA-mATF1 (1×10^7 PFU/ml per virus) for 48 h. Cell extracts were prepared in NP-40 lysis buffer and coimmunoprecipitation was performed as described above.

ChIP assay. The chromatin immunoprecipitation (ChIP) assay was performed with a kit according to the manufacturer's instructions (EMD Millipore). The antibodies used for ChIP assays of HSF1, ATF1/CREB, phosphorylated ATF1-Ser63/CREB-Ser133, CREM, p300, and CBP are described above in the section on RNA interference, and that used for ChIP assay of BRG1 was anti-SNF2b/BRG1 (07-478; Millipore). To immunoprecipitate ATF1 specifically, we constructed the bacterial expression vector pET21a-mATF1-His by inserting an EcoRI/XhoI fragment of pcDNA4-HA-mATF1 into the pET21a vector (Novagen) and generated rabbit antiserum against recombinant mouse ATF1-His (anti-mATF1-1). To examine active chromatin marks, we used antibodies to histone H3 (ab1791, lot no. GR135171-1; Abcam), H3K27Ac (ab4729, lot no. GR124541-1), and H3K9Ac (07-352, lot no. 2325091; Millipore). Real-time qPCR of ChIP-enriched DNAs was performed with primers described previously (19) and those listed in Table S3 in the supplemental material. The percentage of the input was determined by comparing the cycle threshold value of each sample to a standard curve generated from a five-point serial dilution of the genomic input and compensated by values obtained with normal IgG. IgG-negative control immunoprecipitations for all sites yielded <0.05% of the input. All reactions were performed in triplicate with samples derived from three experiments.

ChIP-seq data analysis. Sequenced reads obtained by performing ChIP sequencing (ChIP-seq) (see Materials and Methods in the supplemental material) were mapped to the mouse genome (UCSC mm9) with Bowtie (26) version 0.12.7, allowing three mismatches in the first 28 bases per read (−n3 option). We only considered uniquely mapped reads and redundantly mapped reads (reads starting exactly at the same 5′ sequence ends) were filtered out for further analysis. Mapping statistics are summarized in Table S4 in the supplemental material. For peak calling and data visualization, we used DROMPA (27) version 1.4.1 with a default parameter set that identified the regions that satisfied the following criteria: >3.0-fold enrichment (ChIP/input), $P < 1 \times 10^{-4}$, and a normalized peak intensity of >6.0. To compare multiple ChIP-seq data, ChIP and input reads were both normalized to the total number of mapped reads per chromosome. MA plots (log ratios [M] versus mean averages [A]) were created by using the CI command of DROMPA version 2.2.5.

Statistical analysis. Data were analyzed with the Student t test or subjected to analysis of variance (ANOVA). Error bars represent the standard deviations (SD) of at least three independent experiments.

ChIP-seq accession number. ChIP-seq data from this study have been deposited in the Sequence Read Archive database (http://www.ncbi.nlm.nih.gov/sra) under accession number SRP037746.

RESULTS

The HSF1-ATF1 complex promoted *HSP70* expression during heat shock. We examined the complex formation of HSF1 and ATF1 and found that HSF1 was coprecipitated with ATF1 in both control and heat-shocked MEF cell extracts to the same level, while ATF1 was similarly coprecipitated with HSF1 (Fig. 1A). HSF1 mobility on SDS-PAGE was retarded because of hyperphos-

FIG 3 The HSF1-ATF1 complex recruited BRG1 and p300/CBP. (A) Schematic representation of the mouse *HSP70.3* locus. DNA regions amplified by real-time PCR are shown as numbered gray boxes, and an amplified intergenic region (Inter.) is also shown. (B) HSF1-dependent recruitment of ATF1 to the *HSP70* promoter. MEF cells infected with Ad-sh-mHSF1-KD2 or Ad-sh-SCR were treated without (C) or with heat shock (HS) at 42°C for 30 min. ChIP-qPCR analyses were performed with ATF1/CREB antibody ($n = 3$). (C) ATF1 was not required for the binding of HSF1 to the *HSP70* promoter *in vivo*. Cells were infected with Ad-sh-mATF1-KD2 or Ad-sh-SCR. ChIP-qPCR analyses were performed with HSF1 antibody. (D) ATF1 occupancy in the presence of mutant HSF1 proteins. Cells in which endogenous HSF1 was replaced with each mutant were left untreated (Cont.) or heat shocked at 42°C for 30 min (HS). ChIP-qPCR analyses in the dHSE were performed ($n = 3$). (E) ATF1 was required for the recruitment of coactivator complexes. Cells infected with adenovirus expressing each shRNA were heat shocked at 42°C for the times indicated. ChIP-qPCR analyses in the dHSE were performed with each antibody ($n = 3$). Western immunoblotting (IB) was performed. (F) Occupancy of BRG1 and p300 in the presence of mutant HSF1 proteins. Cells were left untreated (Cont.) or heat shocked at 42°C for 30 min (HS), and ChIP-qPCR analyses were performed with each antibody as described for panel E.

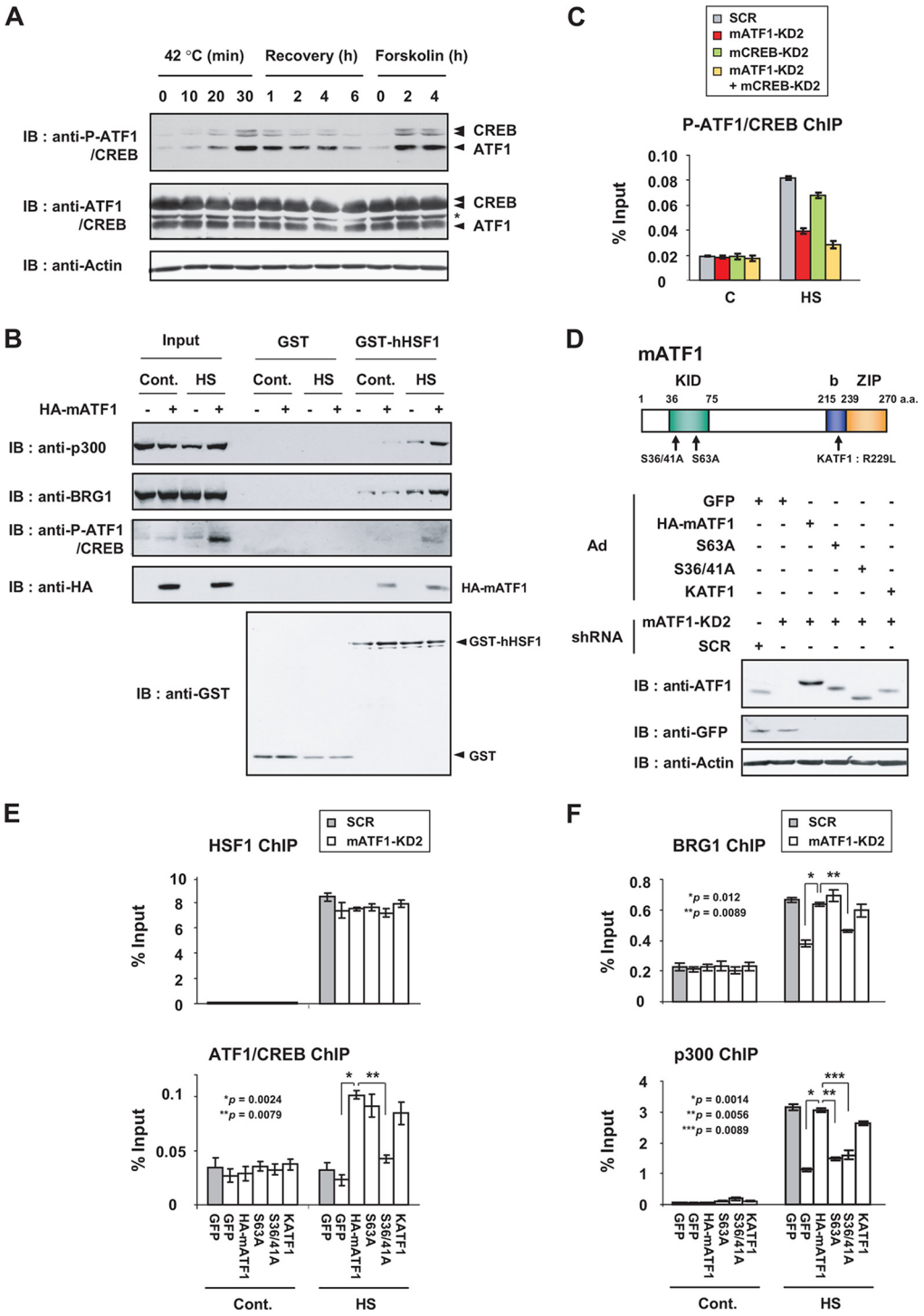

FIG 4 Complex formation depended on ATF1 phosphorylation. (A) Phosphorylation of ATF1-Ser63 was induced during heat shock. MEF cells were heat shocked at 42°C for 30 min and allowed to recover at 37°C for the times indicated or treated with forskolin (20 μM). Cell extracts were subjected to Western immunoblotting (IB) with phospho-ATF1-Ser63/CREB-Ser133 or ATF1/CREB antibody. Arrowheads indicate the positions of the proteins, and the asterisk shows the position of nonspecific bands. (B) Heat shock markedly induced the interaction between the HSF1-ATF1 complex and p300. Cells in which endogenous ATF1 was replaced with HA-mATF1 were left untreated (Cont.) or heat shocked (HS) at 42°C for 30 min. GST pulldown from mixtures of purified GST or GST-hHSF1 with the cell extracts was performed and immunoblotted with each antibody. (C) Occupancy of phosphorylated ATF1-Ser63. Cells were infected with each adenovirus expressing a specific shRNA and heat shocked at 42°C for 30 min. ChIP-qPCR analyses in the dHSE of the *HSP70* promoter were performed with phospho-ATF1-Ser63/CREB-Ser133 antibody ($n = 3$). (D) Replacement of endogenous ATF1 with each mutant protein. Schematic representation of mutant mATF1 proteins. b, basic region; ZIP, leucine zipper. Endogenous ATF1 was replaced with each HA-tagged mutant mATF1 protein, including HA-KATF1 (R229L). Levels of wild-type and mutated mATF1 were examined by Western blotting. (E) Recruitment of ATF1 in the *HSP70* promoter depends on its phosphorylation at Ser36/41. After endogenous ATF1 was replaced with each mutant protein, cells were left untreated (Cont.) or heat shocked (HS) at 42°C for 30 min. ChIP-qPCR analyses were performed on the dHSE of the *HSP70* promoter ($n = 3$). (F) Effects of ATF1 phosphorylation at Ser36/41 or Ser63 on the recruitment of BRG1 and p300 on the *HSP70* promoter. After endogenous ATF1 was replaced with each mutant protein, cells were heat shocked and ChIP-qPCR analyses were performed.

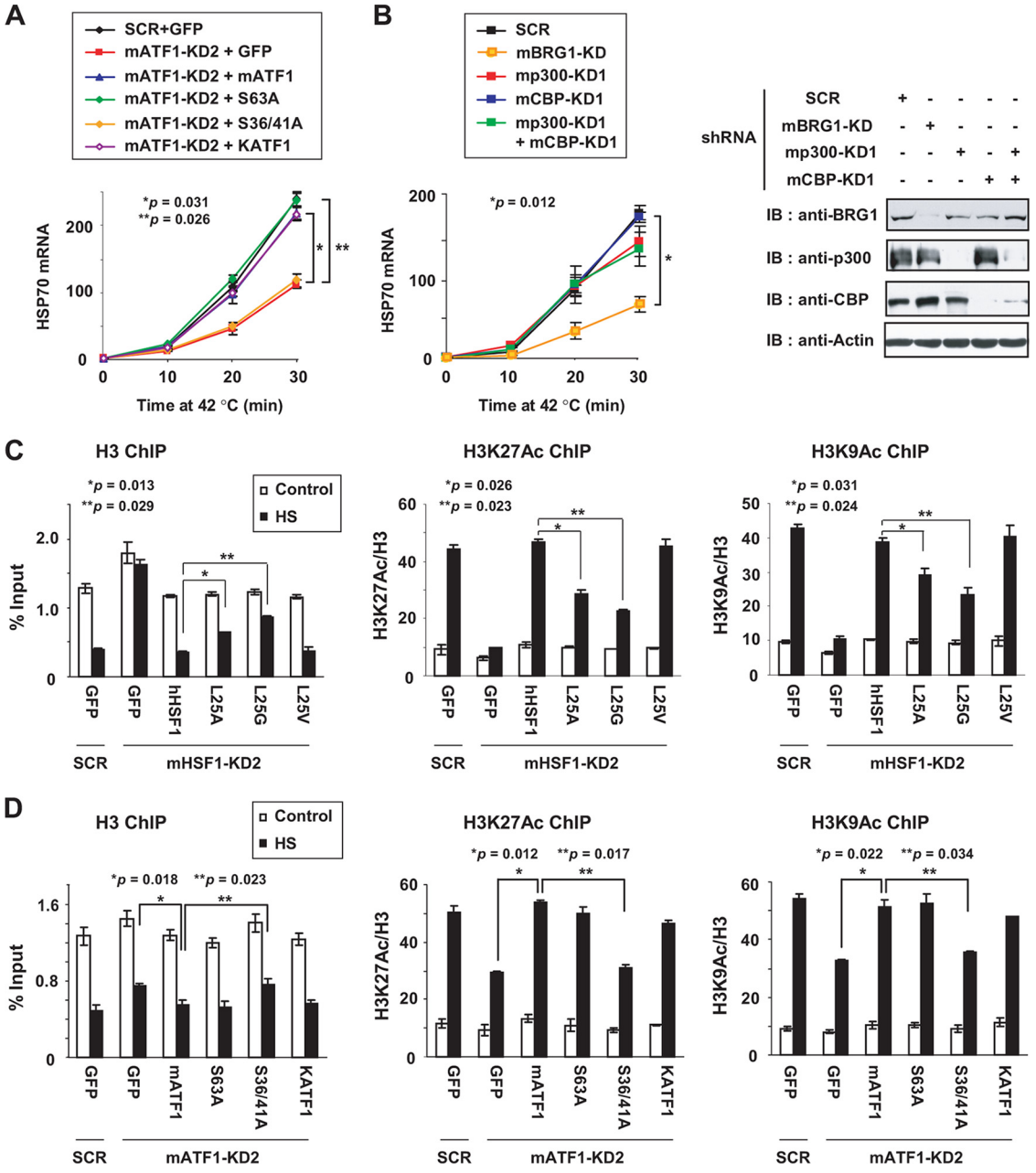

FIG 5 Recruitment of BRG1 but not p300/CBP facilitated the establishment of an active chromatin state during heat shock. (A) Phosphorylation of ATF1-Ser36/41 was required for *HSP70* expression. Endogenous ATF1 was replaced with each mutant protein in MEF cells. *HSP70* mRNA levels during heat shock at 42°C for the times indicated were quantified by RT-qPCR. The level of *HSP70* mRNA in control Ad-sh-SCR-infected cells was defined as 1, and relative levels are shown ($n = 3$). (B) Knockdown of BRG1 reduced the expression of *HSP70* mRNA. Cells were infected with adenoviruses expressing p300 and CBP. *HSP70* mRNA levels during heat shock were quantified by RT-qPCR as described for panel A (left). Cell extracts were prepared, and Western immunoblotting (IB) was performed with each antibody (right). (C) Changes observed in the chromatin structure of cells expressing each mutant hHSF1 protein. Cells were infected with Ad-sh-mHSF1-KD2 or Ad-sh-SCR as a control and then infected with adenovirus expressing each mutant hHSF1 protein or GFP. ChIP-qPCR analyses were performed in the dHSE of the *HSP70* promoter with H3 antibody, and the levels of active chromatin marks were analyzed and normalized to histone H3 occupancy. Error bars show the mean ± SD ($n = 3$). *P* values were calculated by ANOVA. (D) Changes in the chromatin structure of cells expressing each mutant mATF1 protein. Cells were infected with Ad-sh-mATF1-KD2 or Ad-sh-SCR as a control and then infected with adenovirus expressing each mutant mATF1 protein or GFP. ChIP-qPCR analyses in the dHSE were performed as described for panel C.

phorylation during heat shock. The DNA-binding domain of HSF1, which was fused to glutathione *S*-transferase (GST) (GST-hHSF1ΔC3), was sufficient to pull down HA-mATF1 (see Fig. S1A in the supplemental material), indicating that ATF1 bound to the HSF1 DNA-binding domain. ATF1 binding was reduced when the N4, N5, or N6 region in the HSF1 DNA-binding domain was deleted, and the binding of hHSF1 lacking the N4 region was more impaired than the others. HA-mATF1 also interacted with hHSF2 and hHSF4 (data not shown). Therefore, we generated and analyzed 16 hHSF1 point mutants in which conserved amino acids in

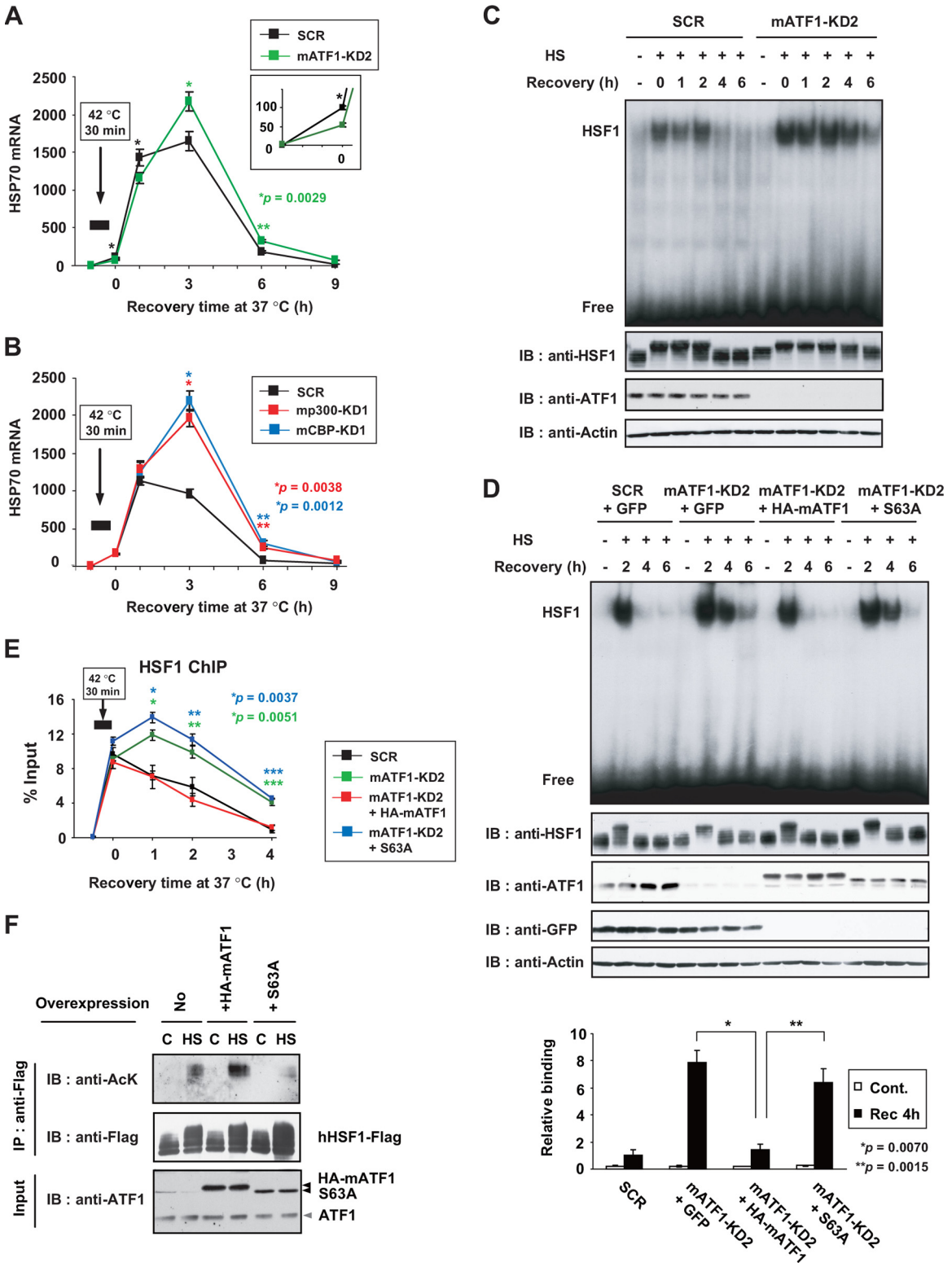

FIG 6 p300/CBP recruitment accelerated the shutdown of HSF1 DNA-binding activity during recovery. (A) Expression of *HSP70* mRNA during recovery in ATF1 knockdown cells. MEF cells that had been infected for 72 h with Ad-sh mATF1-KD2 or Ad-sh-SCR were heat shocked at 42°C for 30 min and then allowed to recover at 37°C for the times indicated. *HSP70* mRNA levels were quantified by RT-qPCR ($n = 3$). The inset shows an enlarged view during heat shock. (B) Expression of *HSP70* mRNA during recovery in p300 or CBP knockdown cells. Cells infected with adenovirus expressing shRNA for p300 or CBP were treated, and *HSP70* mRNA levels were quantified as described for panel A. (C) Sustained *in vitro* DNA-binding activity of HSF1 during recovery in extracts of ATF1 knockdown cells. Cells treated as described for panel A were heat shocked at 42°C for 30 min and then allowed to recover at 37°C for the times indicated. Whole-cell extracts were prepared and subjected to EMSA with a ^{32}P-labeled ideal HSE oligonucleotide (top). Western immunoblotting (IB) was performed

the N4 region were replaced with alanine (Fig. 1B). We found that hHSF1-L25A did not interact with HA-mATF1 but bound to DNA at the same level as wild-type hHSF1 (see Fig. S1B and C). Furthermore, we replaced the leucine at amino acid 25 with other amino acids. hHSF1-L25A and hHSF1-L25G did not interact with ATF1, whereas hHSF1-L25V did (Fig. 1C). All three mutant hHSF1 proteins bound to DNA at similar levels *in vitro* (Fig. 1D). This leucine at amino acid 25 was located in helix 1 of the winged helix-turn-helix (HTH) DNA-binding domain of HSF1 and was evolutionally conserved among all eukaryotic HSF family members, except *Caenorhabditis elegans* (isoleucine) and *Saccharomyces cerevisiae* (methionine) HSF (see Fig. S1D).

To examine the impact of the ATF1/CREB family members on stress-inducible gene expression, we knocked them down in MEFs. The adenovirus vector expressing shRNA for mATF1 (KD1, KD2), mCREB (KD1, KD2), or mCREM (KD1, KD2) efficiently reduced each target gene product (Fig. 2A). We found that ATF1 or CREM knockdown, but not CREB knockdown, reduced the expression of *HSP110*, *HSP70*, and *HSP40* mRNAs during heat shock (Fig. 2B). The knockdown of ATF1 or CREM reduced the expression of *HSP70* mRNA when cells were treated not only with heat shock (HS) but also with sodium arsenite (As), a proline analogue (L-azetidine-2-carboxylic acid, AzC), or a proteasome inhibitor (MG132) (Fig. 2C). Furthermore, the induction of *HSP70* mRNA was also reduced in ATF1-null MEF cells, and the overexpression of HA-tagged mouse ATF1 (HA-mATF1) or HA-mCREM in ATF1-null cells, but not that of HA-mCREB, restored the expression of *HSP70* (Fig. 2D). Thus, ATF1 and CREM were required for the induction of *HSP70* expression in response to various stresses in MEF cells. We analyzed the effects of the HSF1-ATF1 interaction on the expression of *HSP70* in more detail and found that replacement with hHSF1-L25A or hHSF1-L25G but not with hHSF1-L25V reduced the expression of *HSP70* mRNA during heat shock (Fig. 2E). Therefore, we concluded that the HSF1-ATF1 complex promoted *HSP70* expression during heat shock.

The HSF1-ATF1 complex was required for the recruitment of coactivator complexes. We examined the effects of ATF1 on the *in vitro* DNA-binding activity of HSF1 by electrophoretic mobility shift assay (EMSA) and found that the knockdown of ATF1 slightly increased HSF1 DNA-binding activity during heat shock (see Fig. S2A in the supplemental material). The ATF1 antibody did not supershift HSF1 activity, unlike the HSF1 antibody, even when ATF1 was overexpressed (see Fig. S2B), suggesting that the HSF1-ATF1 complex may not be stable enough to be detected by EMSA. To reveal the mechanisms by which ATF1 promoted the HSF1-mediated transcription of *HSP70*, we performed ChIP assays of the promoters of mouse *HSP70.3* (also known as *Hspa1a*) with primers for a site including pHSE or dHSE (Fig. 3A) (19). ChIP-qPCR analysis with the ATF1/CREB antibody, which immunoprecipitated both ATF1 and CREB, showed that ATF1/CREB was recruited to the HSEs during heat shock (Fig. 3B). ATF1 was detected dominantly in the dHSE in heat-shocked MEF cells (see Fig. S2C). HSF1 knockdown markedly reduced the occupancy of ATF1/CREB on the HSEs (Fig. 3B). HSF1 binding was not affected by ATF1 knockdown (Fig. 3C). CREM was also recruited to the dHSE during heat shock in a manner that was dependent on HSF1 (see Fig. S2D). Furthermore, ATF1/CREB occupancy on the dHSE during heat shock was markedly reduced in cells in which endogenous HSF1 was replaced with hHSF1-L25A or hHSF1-L25G (Fig. 3D). These results demonstrated that HSF1 recruited ATF1 on the *HSP70* promoter.

Transcription factor binding to its regulatory elements generally recruits coactivator complexes including chromatin-modifying enzymes and chromatin-remodeling complexes (28, 29), and HSF1 was previously shown to recruit BRG1, a component of chromatin-remodeling complexes (21), and the lysine acetyltransferase p300 (KAT3B) (22). The necessity of the former for *HSP70* expression during heat shock has been reported in mammalian cells (30). Therefore, we investigated the recruitment of coactivator complexes and found that BRG1 and p300 (KAT3B) were robustly recruited to the dHSE in the *HSP70* promoter during heat shock for 30 min, whereas the recruitment of CBP (KAT3A) peaked 5 min after heat shock and then rapidly decreased (Fig. 3E). ATF1 knockdown significantly reduced the recruitment of all of these components. Furthermore, the recruitment of BRG1 and p300 on the dHSE during heat shock was reduced by the replacement of endogenous HSF1 with hHSF1-L25A or hHSF1-L25G (Fig. 3F). Thus, the HSF1-ATF1 complex was necessary for the maximal recruitment of coactivators during heat shock.

HSF1 transcription complex formation depended on ATF1 phosphorylation. A previous study reported that ATF1 was phosphorylated at Ser63 by cyclic AMP (cAMP)-dependent protein kinase (PKA), similar to CREB and CREM, and phosphorylated ATF1-Ser63 recruited p300/CBP (23). We investigated this modification and found that ATF1 was markedly phosphorylated at Ser63 in MEF cells in response to stresses including heat shock and proteasome inhibition, while CREB at Ser133 was modestly phosphorylated (Fig. 4A; see Fig. S3A and B in the supplemental material). The phosphorylated levels of ATF1 during heat shock were low in other cell lines, such as HeLa and 293, whereas those of CREB were high. Pulldown assay revealed that both ATF1 and p300 expressed in control cells were coprecipitated with GST-hHSF1 (Fig. 4B). The coprecipitation of p300 with GST-hHSF1 was markedly greater in heat-shocked cells than in control cells, whereas ATF1 in heat-shocked cells was coprecipitated at the same

(bottom). (D) Reductions in HSF1 DNA-binding activity during recovery were delayed in cells expressing mutant mATF1 proteins. Cells were infected with Ad-sh-mATF1-KD2 or Ad-sh-SCR and then infected with adenovirus expressing HA-mATF1, HA-mATF1-S63A, or GFP. These cells were heat shocked, and an EMSA was performed as described for panel C (top). HSF1 binding in extracts from control cells (Cont.) and cells allowed to recover for 4 h was quantified by using NIH Image ($n = 3$) (bottom). The level of HSF1 binding in Ad-sh-SCR-infected cells that recovered from heat shock was defined as 1, and relative levels are shown. (E) Sustained binding of HSF1 *in vivo* to the *HSP70* promoter during recovery in cells expressing mutant mATF1 proteins. Cells were treated as described for panel D. ChIP-qPCR analyses were performed with HSF1 antibody ($n = 3$). (F) ATF1 promoted the acetylation of HSF1. The vector pcDNA4/HisMax (No), an expression vector for HA-mATF1 (+HA-mATF1) or HA-mATF1-S63A (+S63A), and those for hHSF1-Flag and p300 were transfected into HEK293 cells. Lysates were prepared from these cells, which were treated without (C) or with heat shock (HS) at 42°C for 1 h. hHSF1-Flag was immunoprecipitated with anti-Flag antibody and blotted with anti-acetylated-lysine antibody (anti-AcK) or anti-Flag antibody. Cell extracts were also subjected to Western blotting with anti-ATF1 antibody (anti-mATF1-1).

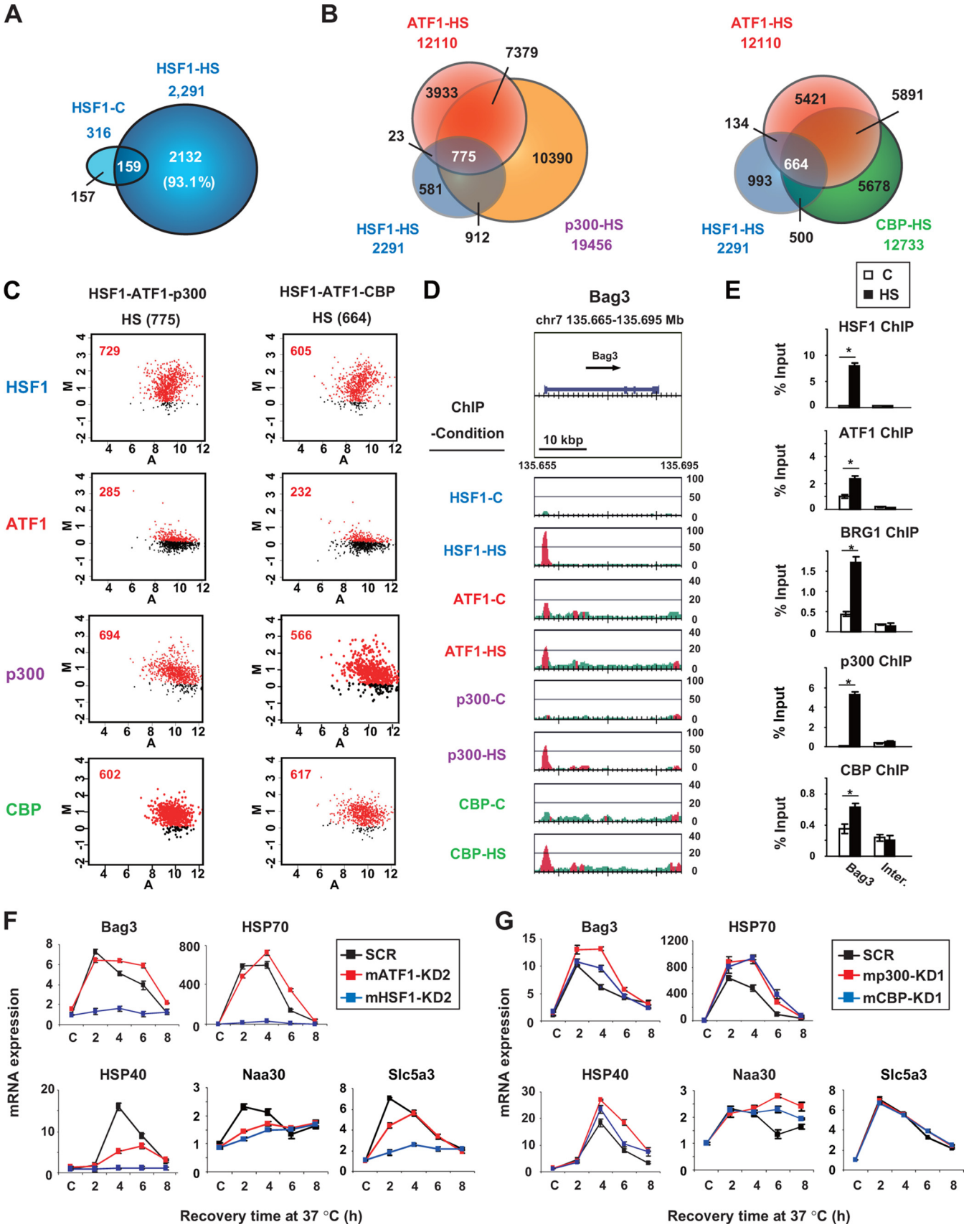
A
HSF1-HS
2,291
HSF1-C
316
159
2132
(93.1%)
157
B
ATF1-HS
12110
7379
3933
23
775
10390
581
HSF1-HS
2291
912
p300-HS
19456
ATF1-HS
12110
5421
5891
134
664
993
5678
HSF1-HS
2291
500
CBP-HS
12733
C
HSF1-ATF1-p300
HS (775)
HSF1-ATF1-CBP
HS (664)
HSF1
ATF1
p300
CBP
729
605
285
232
694
566
602
617
M
A
D
Bag3
chr7 135.665-135.695 Mb
Bag3
10 kbp
135.655
135.695
ChIP
-Condition
HSF1-C
HSF1-HS
ATF1-C
ATF1-HS
p300-C
p300-HS
CBP-C
CBP-HS
E
C
HS
HSF1 ChIP
ATF1 ChIP
BRG1 ChIP
p300 ChIP
CBP ChIP
% Input
Bag3
Inter.
F
Bag3
HSP70
HSP40
Naa30
Slc5a3
SCR
mATF1-KD2
mHSF1-KD2
mRNA expression
Recovery time at 37 °C (h)
G
Bag3
HSP70
HSP40
Naa30
Slc5a3
SCR
mp300-KD1
mCBP-KD1
mRNA expression
Recovery time at 37 °C (h)

level. Furthermore, phosphorylated ATF1-Ser63 was markedly recruited on the *HSP70* promoter during heat shock (Fig. 4C).

We searched for the region of ATF1 that is required for its interaction with HSF1 and found that HA-mATF1 lacking a kinase-inducible domain (KID) (HA-mATF1ΔKID) did not interact with HSF1 in HEK293 cells (see Fig. S3C in the supplemental material). The N-terminal region (amino acids 36 to 42) in the KID was required for this interaction (Kmu1), whereas the C-terminal region (amino acids 63 to 74) including Ser63 was not (Kmu4) (see Fig. S3D). The former contained Ser36 and Ser41, which were constitutively phosphorylated by casein kinases 1 and 2 (31). Their replacement with alanine (HA-mATF1-S36/41A) abolished the interaction with HSF1 (see Fig. S3D and E), indicating that the constitutive phosphorylation of ATF1 at Ser36 and Ser41 was required for its interaction with HSF1.

We next examined the HSF1 transcription complex *in vivo* in the presence of these mutant ATF1 proteins. Endogenous ATF1 was replaced with ectopically expressed HA-mATF1 or each mutant protein in MEF cells (Fig. 4D). ChIP-qPCR showed that HA-mATF1-S36/41A did not occupy the dHSE in the *HSP70* promoter during heat shock and also did not recruit BRG1 or p300 at maximal levels (Fig. 4E and F). In contrast, HA-mATF1-S63A occupied the dHSE during heat shock and recruited BRG1, although it did not recruit p300. BRG1 and p300 were still recruited on the *HSP70* promoter at low levels even in the presence of these mutant ATF1 proteins. HA-KATF1, which did not directly bind to DNA (32), occupied the dHSE during heat shock and recruited BRG1 and p300, which excluded the possibility that ATF1 directly bound to DNA. These results demonstrated that the formation of the HSF1 transcription complex depended partly on the phosphorylation of ATF1 at Ser36/41 and Ser63.

ATF1-BRG1 facilitated the establishment of an active chromatin state during heat shock. The heat shock-induced expression of *HSP70* mRNA in ATF1 knockdown cells was restored by the overexpression of HA-mATF1-S63A, as well as HA-mATF1 or HA-KATF1, but not by the overexpression of HA-mATF1-S36/41A (Fig. 5A). Therefore, we knocked down coactivators and found that BRG1 knockdown reduced the induction of *HSP70* mRNA, whereas the knockdown of p300, CBP, or both did not affect *HSP70* expression during heat shock at 42°C until 30 min (Fig. 5B). As a control, we observed a significant reduction in the forskolin-mediated induction of AREG mRNA in p300 and CBP knockdown cells (see Fig. S4A in the supplemental material) (33).

Since p300/CBP can acetylate histones (10), we examined active chromatin marks. Heat shock reduced the occupancy of histone H3 on the *HSP70* promoter and elevated active chromatin marks such as the acetylation of H3K27 and H3K9 (see Fig. S4B). BRG1 knockdown impaired the heat shock-induced reduction in histone H3 occupancy and elevation in the active chromatin marks. However, the knockdown of p300 or CBP did not affect these chromatin marks. When endogenous HSF1 was replaced with hHSF1-L25A or hHSF1-L25G or endogenous ATF1 was replaced with HA-mATF1-S36/41A, the heat shock-induced reduction in the histone H3 occupancy and elevation in active chromatin marks were impaired (Fig. 5C and D). The replacement of endogenous ATF1 with HA-mATF1-S63A again had no effect on chromatin marks during heat shock (Fig. 5D). Taking these findings together, we concluded that HSF1-ATF1 complex-mediated recruitment of BRG1 but not p300/CBP promoted the establishment of the active chromatin state of the *HSP70* promoter during heat shock.

ATF1-p300/CBP accelerated the shutdown of HSF1 DNA-binding activity during recovery from acute stress. To elucidate the roles of the stress-inducible recruitment of p300 and CBP in the HSF1 transcription complex, we examined the profiles of *HSP70* mRNA expression during recovery from acute stress. Although *HSP70* mRNA levels were markedly lower in ATF1 knockdown MEF cells than in scrambled-RNA-expressing cells during heat shock at 42°C for 30 min (Fig. 6A, inset), they were higher in ATF1 knockdown cells, as well as in CREB or CREM knockdown cells, 3 h after heat-shocked cells had recovered at 37°C (Fig. 6A; see Fig. S5A in the supplemental material). Furthermore, *HSP70* mRNA levels were markedly higher in p300 or CBP knockdown cells during recovery (Fig. 6B). Thus, ATF1, p300, and CBP promoted the shutdown of *HSP70* expression during recovery from acute stress.

We next investigated whether the recruited p300 and CBP regulated the DNA-binding activity of HSF1 because the acetylation of HSF1 has been shown to impair its DNA-binding activity (34). The *in vitro* DNA-binding activity of HSF1 during recovery at 37°C continued to be markedly higher in whole-cell extracts from ATF1 knockdown cells or p300 or CBP knockdown cells than in those from scrambled-RNA-expressing cells (Fig. 6C; see Fig. S5B). Furthermore, the replacement of endogenous ATF1 with HA-mATF1-S63A elevated its DNA-binding activity at 4 h during recovery (Fig. 6D). HSF1 binding to the *HSP70* promoter *in vivo* continued to be higher in cells expressing HA-mATF1-S63A (Fig. 6E). We examined the acetylation status of ectopically expressed hHSF1-Flag and showed that HSF1 was acetylated more in heat-shocked HEK293 cells overexpressing HA-mATF1 than in those overexpressing none, whereas it was acetylated less in those overexpressing HA-mATF1-S63A (Fig. 6F). The acetylation of endogenous HSF1 was not detected. These results demonstrated that the ATF1-mediated recruitment of p300/CBP accelerated the shut-

FIG 7 ATF1 occupied the promoters of many HSF1 targets during heat shock and modulated their expression. (A) Venn diagram of HSF1 ChIP-seq binding peaks in control (HSF1-C) and heat-shocked (HSF1-HS) MEF cells. Numbers of binding peaks are indicated. (B) Venn diagram of ChIP-seq binding peaks for HSF1, ATF1, and p300/CBP in heat-shocked cells. (C) MA plots of ChIP-seq binding intensities for HSF1, ATF1, p300, and CBP in control (R_1) and heat-shocked cells (R_2) at the common binding peaks for HSF1-HS/ATF1-HS/p300-HS (775 peaks) or HSF1-HS/ATF1-HS/CBP-HS (664 peaks). The M and A values of each peak were calculated and plotted, where $M = \log_2(R_1/R_2)$ and $A = \log_2(R_1 + R_2)/2$. Numbers of red dots whose ratios (M) increased during heat shock ($-\log_{10}P > 1$) are indicated. (D) ChIP-seq binding profiles of HSF1, ATF1, p300, and CBP at the *Bag3* locus in control (C) and heat-shocked (HS) cells. Normalized read numbers are shown. Significantly enriched regions identified as peaks are in red. The arrow indicates the 5′-to-3′ orientation of each gene. (E) Recruitment of the HSF1-ATF1 complex on the *Bag3* promoters of target genes. MEF cells were left untreated (C) or heat shocked (HS) at 42°C for 30 min. ChIP-qPCR analyses of each promoter were performed with HSF1, ATF1 (αmATF1-1), BRG1, p300, or CBP antibody ($n = 3$). (F) Expression of HSF1 target genes in ATF1 knockdown cells. MEF cells that were infected for 72 h with Ad-sh-mATF1-KD2, Ad-sh-mHSF1-KD2, or Ad-sh-SCR were heat shocked at 42°C for 30 min and allowed to recover at 37°C for the times indicated. mRNA levels were quantified by RT-qPCR ($n = 3$). (G) Expression of HSF1 target genes in p300 and CBP knockdown cells. Cells infected for 72 h with Ad-sh-mp300-KD1, Ad-sh-mCBP-KD1, or Ad-sh-SCR were treated and analyzed as described for panel F.

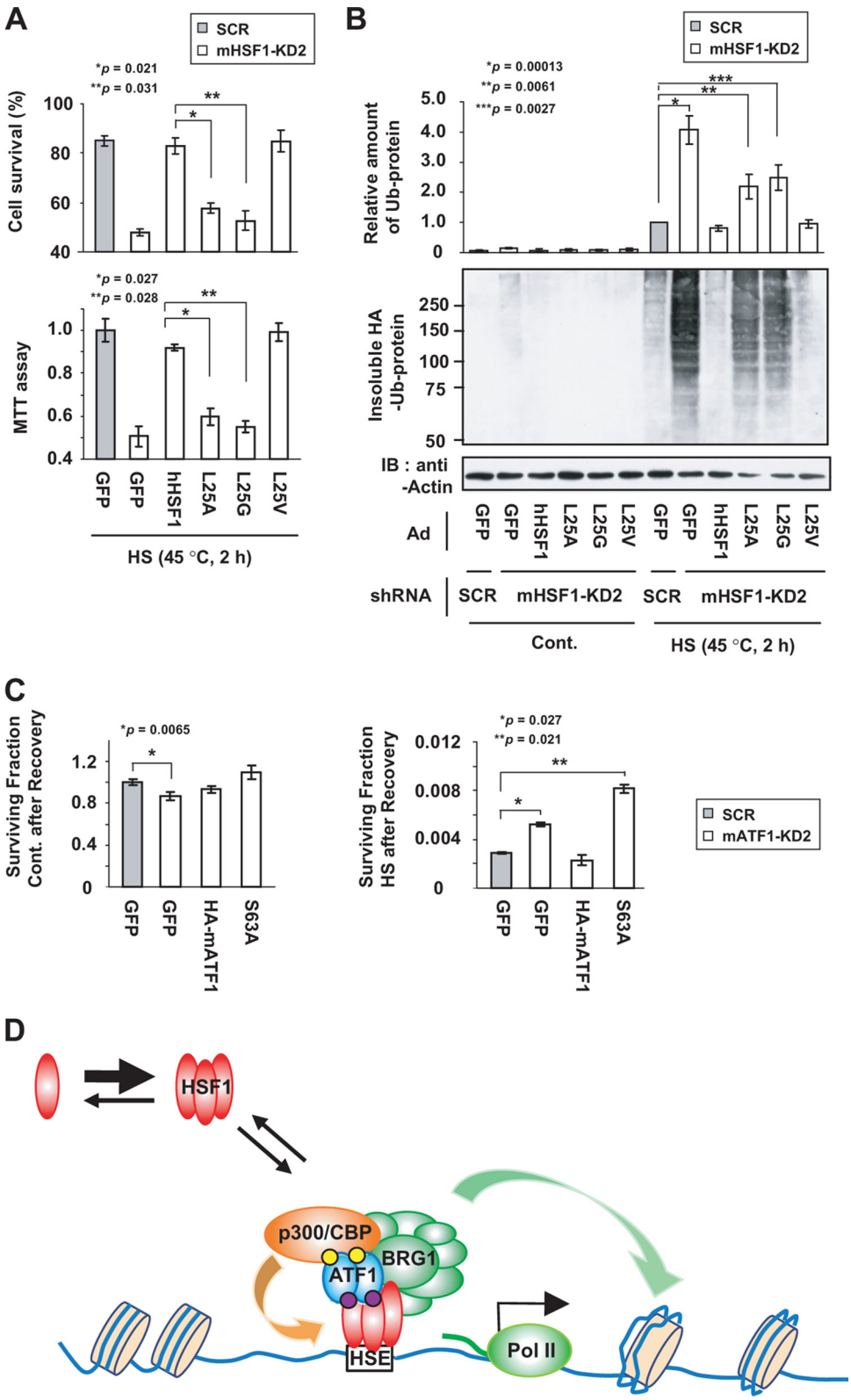

FIG 8 The HSF1-ATF1 complex modulated resistance to heat shock. (A) HSF1-ATF1 complex was required for cell survival. MEF cells were infected with Ad-sh-mHSF1-KD2 or Ad-sh-SCR for 24 h and then infected with each adenoviral expression vector for 48 h. After the cells had been incubated at 45°C for 2 h, the viable cells excluding trypan blue were counted (top) and a 3-(4,5-dimethyl-2-thiazolyl)-2,5-diphenyl-2H-tetrazolium bromide (MTT) assay was performed (bottom) ($n = 3$). (B) The HSF1-ATF1 complex elevated the accumulation of ubiquitylated (Ub) proteins. Cells treated as described for panel A were infected with Ad-HA-Ub for 2 h, maintained with normal medium at 37°C for 22 h, and then left untreated (Cont.) or heat shocked (HS) at 45°C for 2 h. Accumulation of insoluble ubiquitylated proteins was examined by Western immunoblotting (IB) with anti-HA antibody and quantified ($n = 3$). β-Actin levels in the soluble

down of HSF1 DNA-binding activity during recovery, possibly through the acetylation of HSF1.

ATF1 occupied the promoters of many HSF1 targets and modulated their expression. We next examined the HSF1-ATF1 complex on the whole genome in MEF cells by performing ChIP-seq analysis with antibodies, including an ATF1-specific antibody. As was reported previously with human cells (35, 36), a weak but distinct HSF1-binding peak was observed in the *HSP70.1* (*HSPA1B*) promoter, which was markedly increased during heat shock (see Fig. S6C in the supplemental material). We identified 316 HSF1 binding sites in control cells and 2,291 in heat-shocked cells, 159 of which were detected under both conditions (Fig. 7A). ATF1, p300, and CBP bound to 12,109, 11,965, and 5,389 sites, respectively, in control cells. Heat shock induced large numbers of new binding sites for p300 and CBP (50.0 and 66.4%, respectively), whereas it induced a limited number of new ATF1 binding sites (20.3%) (see Fig. S6A). p300 and CBP bound considerably to the same sites (86.8%) in heat-shocked cells (see Fig. S6B). A comparison of these binding sites showed that 775 sites (34.0%) of the heat-inducible 2,132 HSF1 binding sites (HSF1-HS) were occupied by ATF1 and p300, while 664 sites (29.0%) were cooccupied by ATF1 and CBP (Fig. 7B). Thus, the genome-wide analysis revealed the prominent cooccupancy of HSF1 with ATF1 on targets during heat shock.

To quantify the intensities of peaks, we generated MA plots of control and heat-shocked binding intensities at the common HSF1-ATF1-p300/CBP binding sites. The binding intensities of HSF1, p300, and CBP at most binding sites were markedly elevated during heat shock, whereas that of ATF1 was moderately increased at 285 and 232 sites (Fig. 7C, red). We found some gene loci near these heat-inducible ATF1 binding sites, such as *Bag3*, *Dnajb1* (*HSP40*), *Naa30*, and *Slc5a3* loci (Fig. 7D and E; see Fig. S6C). HSF1, ATF1, p300, and CBP cooccupied these promoters under heat shock conditions. ATF1 peaks (in red) were detected only in heat-shocked cells (*Naa30* and *Slc5a3*) or in both control and heat-shocked cells (*Bag3* and *Dnajb1*). They were also detected at the *Hspa1a*/*Hspa1b* (*HSP70*) locus in both control and heat-shocked cells but were hardly increased during heat shock (see Fig. S6C). Although elevations in ATF1 binding intensities during heat shock at these gene loci were generally low in ChIP-seq data, we confirmed by using ChIP-qPCR that ATF1 occupancy moderately increased during heat shock at the promoters of these HSF1 targets in a manner that was dependent on HSF1 (see Fig. S6D and E). Furthermore, the recruitment of BRG1, p300, or CBP required ATF1 at different levels in these promoters (see Fig. S6F).

We also examined the expression of the HSF1 targets when cells were heat shocked at 42°C for 30 min and then recovered at 37°C for 8 h. ATF1 knockdown delayed the shutdown of *Bag3* expression, as well as that of *HSP70*, whereas it markedly suppressed the expression of *HSP40*, *Naa30*, and *Slc5a3*, and this may be due in part to the insufficient recruitment of BRG1 (Fig. 7F). Furthermore, the knockdown of p300 or CBP delayed the shutdown of all expression, except for that of Slc5a3. These results indicated that ATF1 modulated the expression of many HSF1 targets during heat shock or recovery.

ATF1 modulated resistance to heat shock. The altered expression of HSF1 target genes, including *HSP* and non-*HSP* genes, may be associated with changes in the proteostasis capacity of cells (20). We showed that cell survival was markedly reduced by the knockdown of HSF1 during extreme heat shock at 45°C and was also moderately reduced by that of ATF1 or BRG1 (see Fig. S7A in the supplemental material). In contrast, the knockdown of p300 or CBP did not affect cell survival of a single exposure to heat shock (see Fig. S7B). The replacement of endogenous HSF1 with hHSF1-L25A or hHSF1-L25G or of endogenous ATF1 with HA-mATF1-S36/41A consistently resulted in decreased cell survival, whereas the replacement of endogenous ATF1 with HA-mATF1-S63A did not affect survival (Fig. 8A; see Fig. S7C). Furthermore, reductions in cell survival were associated with the elevated accumulation of ubiquitylated misfolded proteins within the cells (Fig. 8B; see Fig. S7D), which suggested that proteostasis capacity may be impaired. We next examined cell survival during the recovery phase by using a colony formation assay. Since cell proliferation was markedly reduced in MEF cells lacking p300 and CBP (37), we examined the survival of cells in which endogenous ATF1 was replaced with HA-mATF1-S63A. We found that cell survival after a second extreme heat shock at 45.5°C, during recovery at 37°C from the first moderate heat shock (42°C, 30 min), was increased in the presence of HA-mATF1-S63A (Fig. 8C). These results showed that ATF1 modulated resistance to heat shock, possibly through the regulation of proteostasis capacity.

DISCUSSION

The rapid induction of gene expression is initially achieved by the binding of transcriptional activators to specific DNA sequences in response to stimuli and is then followed by the recruitment of coactivator complexes including chromatin-modifying enzymes and nucleosome-remodeling complexes. These early steps in the transcription cycle are known as activator-dependent recruitment and are the most important for inducible gene expression (10). These steps result in the formation of preinitiation complexes including Pol II and the release of paused Pol II into productive elongation (12). Previous studies demonstrated that the binding of an active HSF1 trimer during heat shock was markedly increased on the *HSP70* promoter and recruited p300 and the SWI/SNF complex including BRG1 in mammalian cells (21, 22). In this study, we showed that ATF1 interacted with the N-terminal DNA-binding domain of HSF1 (see Fig. S1A in the supplemental material), partly through an evolutionally conserved leucine at amino acid 25, located in the winged HTH motif (Fig. 1B). This interac-

fraction are also shown. Ad, adenovirus. (C) Impaired recruitment of p300 or CBP resulted in increased cell survival of the second heat shock during recovery from the first. Cells were infected with Ad-sh-mATF1-KD2 or Ad-sh-SCR for 24 h and then infected with Ad-GFP, Ad-HA-mATF1, or Ad-HA-mATF1-S63A for 48 h. Cells were heat shocked at 42°C for 30 min and allowed to recover at 37°C for 4 h. These cells (left) and cells incubated for a further 1 h at 45.5°C (right) were inoculated into new dishes, and the colonies (>20 cells) were counted on day 7. The colony number against the total number of inoculated cells is shown as the surviving fraction ($n = 3$). (D) Schematic model showing the formation of the HSF1-ATF1 transcription complex, which affects chromatin structures and HSF1 DNA-binding activities. HSF1 recruits ATF1, which accelerates the recruitment of p300, CBP, and the BRG1-containing chromatin remodeling complex. BRG1 facilitates the establishment of an active chromatin state in HSF1 target genes, whereas p300 and CBP inactivate HSF1 DNA-binding activity. Purple and yellow circles indicate phosphorylated Ser36/41 and Ser63 in ATF1, which are required for the interaction with HSF1 and p300/CBP, respectively. CREB and CREM are also recruited by HSF1.

tion facilitated the HSF1-mediated recruitment of SWI/SNF on the *HSP70* promoter during heat shock (Fig. 3), promoted the establishment of an active chromatin state, and supported the optimal induction of *HSP70* expression during heat shock (Fig. 2 and 5, model in Fig. 8D). The HSF1-ATF1 complex not only modulated the expression of *HSP70* but also the products of many HSF1 target genes. Although the induction of some targets, including *HSP70*, was reduced moderately in the absence of ATF1, that of others, such as *HSP40*, was highly dependent on ATF1 (Fig. 7). These results may explain why ATF1 markedly contributed to resistance to detrimentally high temperatures in mammalian cells (Fig. 8A and B).

ATF1 was also involved in the HSF1-mediated recruitment of the chromatin-modifying enzymes p300 and CBP on the *HSP70* promoter during heat shock (Fig. 3). These KATs were shown to be enriched in active genes and were correlated with gene expression in the whole genome (38). Furthermore, previous studies suggested that p300 may promote heat-inducible *HSP70* expression in *Xenopus* oocytes and mammalian cells (22, 39). As shown in Fig. 8D, we demonstrated that the recruitment of p300 on the *HSP70* promoter depended on the phosphorylation of ATF1 at Ser63, which was markedly induced during heat shock (Fig. 4A). However, neither p300 nor CBP affected active histone marks, including histone acetylation on the *HSP70* promoter or altered *HSP70* expression during heat shock (Fig. 5). Instead, p300 and its *Drosophila* homolog have been suggested to inactivate HSF1 through its acetylation (34, 40, 41). We showed that ATF1 could promote the acetylation of HSF1 and accelerated the shutdown of its DNA-binding activity during recovery (Fig. 6). Shutdown during the recovery period was delayed, even in the presence of p300 and CBP, when endogenous ATF1 was replaced with HA-mATF1-S63A. This result excluded the possibility that the delayed shutdown of HSF1 DNA-binding activity was due to the HSF1-independent roles of p300 and CBP. Although the recruitment of p300/CBP during heat shock was reduced only modestly in the *HSP70* promoter in the absence of ATF1, ATF1 bound to at least one-third of HSF1-binding sites and accelerated their recruitment to most sites at different levels (Fig. 7; see Fig. S6F). Furthermore, ATF1 facilitated the interaction of HSF1 and p300 in the absence of DNA (Fig. 4B). As a result, ATF1-p300/CBP could have profound effects on the inactivation of the DNA-binding activity of intracellular HSF1 during recovery, possibly through the acetylation of HSF1 (Fig. 6).

HSF1 recruited not only ATF1 but also CREB and CREM on the *HSP70* promoter. While CREM promoted *HSP70* expression during heat shock and its shutdown during recovery, similar to ATF1, CREB only accelerated the latter in MEF cells (Fig. 2C; see Fig. S5A). Although the specificity of each ATF1/CREB member for the recruitment of BRG1 and p300/CBP was unclear, all three members modulated the expression of the HSF1 target genes. ATF1/CREB members were previously shown to be activated in response to metabolic signals such as cAMP elevation and played roles in metabolic homeostasis by regulating the expression of genes involved in glucose and lipid metabolism and in mitochondrial function (23). Our results showed that the HSF1 transcription complex was regulated through the phosphorylation status (Ser36/41 and Ser63 in ATF1) and expression levels of ATF1 (Fig. 3 and 4). The former was controlled by various protein kinases, including PKA (23). The latter was also altered in response to stimuli including changes in metabolic homeostasis (42). Previous studies reported that loss of CREM and CREB functions led to neurodegeneration in mice (43), while a mutation in the *Drosophila* homolog of CREB increased the lethality of polyglutamine toxicity (44); however, mice lacking ATF1 showed no overt phenotype (45). These phenotypes may be caused in part by the impaired regulation of HSF1 target gene expression. Our results suggested that various stimuli, including metabolic signals, modulated proteostasis capacity through the regulation of ATF1/CREB members, and therefore, these signals and factors may be potential therapeutic targets for ameliorating age-related protein-misfolding diseases.

The heat shock response is a universal mechanism of adaptation to proteotoxic stress, including heat shock, that is evolutionally conserved in living organisms (2). As a master regulator of this response in all eukaryotes, HSF should be one of the ancient factors that regulate primitive response mechanisms (6, 17). Therefore, it was surprising that stress-inducible formation of the HSF1 transcription complex and induction of heat shock gene expression required other transcription factors, the ATF1/CREB members, involved in metabolic homeostasis. Our results provided a mechanism that regulated stress-inducible HSF1 transcription complex formation and tightly connected proteostasis capacity and metabolic homeostasis and suggest that the complexity of the primitive heat shock response mechanism in cells may have been increased as an adaptation to metabolic changes during evolution.

ACKNOWLEDGMENTS

We thank to Naoko Yokota for data analysis of the ChIP-seq.

This work was supported in part by grants from the Japan Society for the Promotion of Science (R.T., M.F., E.T., N.H., and A.N.), a Grant-in-Aid for Scientific Research on Innovative Areas (Cross Talk between Transcriptional Control and Energy Pathways, Mediated by Hub Metabolites) (A.N.), Takeda Science Foundation Special Project Research (A.N.), the Uehara Science Foundation (M.F.), and the Yamaguchi University Research Project on STRESS (A.N.).

REFERENCES

1. **Balch WE, Morimoto RI, Dillin A, Kelly JW.** 2008. Adapting proteostasis for disease intervention. Science **319:**916–919. http://dx.doi.org/10.1126/science.1141448.
2. **Lindquist S.** 1986. The heat-shock response. Annu Rev Biochem **55:**1151–1191. http://dx.doi.org/10.1146/annurev.bi.55.070186.005443.
3. **Richter K, Haslbeck KM, Buchner J.** 2010. The heat shock response: life on the verge of death. Mol Cell **40:**253–266. http://dx.doi.org/10.1016/j.molcel.2010.10.006.
4. **Morimoto RI.** 2011. The heat shock response: systems biology of proteotoxic stress in aging and disease. Cold Spring Harbor Symp Quant Biol **76:**91–99. http://dx.doi.org/10.1101/sqb.2012.76.010637.
5. **Guisbert E, Yura T, Rhodius VA, Gross CA.** 2008. Convergence of molecular, modeling, and systems approaches for an understanding of the Escherichia coli heat shock response. Microbiol Mol Biol Rev **72:**545–554. http://dx.doi.org/10.1128/MMBR.00007-08.
6. **Wu C.** 1995. Heat shock transcription factors: structure and regulation. Annu Rev Cell Dev Biol **11:**441–469. http://dx.doi.org/10.1146/annurev.cb.11.110195.002301.
7. **Morimoto RI.** 1998. Regulation of the heat shock transcriptional response: cross talk between a family of heat shock factors, molecular chaperones, and negative regulators. Genes Dev **12:**3788–3796. http://dx.doi.org/10.1101/gad.12.24.3788.
8. **Willenbrock H, Ussery DW.** 2004. Chromatin architecture and gene expression in Escherichia coli. Genome Biol **5:**252. http://dx.doi.org/10.1186/gb-2004-5-12-252.
9. **Segal E, Widom J.** 2009. What controls nucleosome positions? Trends Genet **25:**335–343. http://dx.doi.org/10.1016/j.tig.2009.06.002.
10. **Weake VM, Workman JL.** 2010. Inducible gene expression: diverse reg-

ulatory mechanisms. Nat Rev Genet **11:**426–437. http://dx.doi.org/10.1038/nrg2781.
11. **Akerfelt M, Morimoto RI, Sistonen L.** 2010. Heat shock factors: integrators of cell stress, development and lifespan. Nat Rev Mol Cell Biol **11:**545–555. http://dx.doi.org/10.1038/nrm2938.
12. **Adelman K, Lis JT.** 2012. Promoter-proximal pausing of RNA polymerase II: emerging roles in metazoans. Nat Rev Genet **10:**720–731. http://dx.doi.org/10.1038/nrg3293.
13. **Smith ST, Petruk S, Sedkov Y, Cho E, Tillib S, Canaani E, Mazo A.** 2004. Modulation of heat shock gene expression by the TAC1 chromatin-modifying complex. Nat Cell Biol **6:**162–167. http://dx.doi.org/10.1038/ncb1088.
14. **Petesch SJ, Lis JT.** 2012. Activator-induced spread of poly(ADP-ribose) polymerase promotes nucleosome loss at Hsp70. Mol Cell **45:**64–74. http://dx.doi.org/10.1016/j.molcel.2011.11.015.
15. **Zobeck KL, Buckley MS, Zipfel WR, Lis JT.** 2010. Recruitment timing and dynamics of transcription factors at the Hsp70 loci in living cells. Mol Cell **40:**965–975. http://dx.doi.org/10.1016/j.molcel.2010.11.022.
16. **Petesch SJ, Lis JT.** 2012. Overcoming the nucleosome barrier during transcript elongation. Trends Genet **28:**285–294. http://dx.doi.org/10.1016/j.tig.2012.02.005.
17. **Fujimoto M, Nakai A.** 2010. The heat shock factor family and adaptation to proteotoxic stress. FEBS J **277:**4112–4125. http://dx.doi.org/10.1111/j.1742-4658.2010.07827.x.
18. **Hayashida N, Fujimoto M, Nakai A.** 2011. Transcription factor cooperativity with heat shock factor 1. Transcription **2:**91–94. http://dx.doi.org/10.4161/trns.2.2.14962.
19. **Fujimoto M, Takaki E, Takii R, Tan K, Prakasam R, Hayashida N, Iemura S, Natsume T, Nakai A.** 2012. RPA assists HSF1 access to nucleosomal DNA by recruiting histone chaperone FACT. Mol Cell **48:**182–194. http://dx.doi.org/10.1016/j.molcel.2012.07.026.
20. **Hayashida N, Fujimoto M, Tan K, Prakasam R, Shinkawa T, Li L, Ichikawa H, Takii R, Nakai A.** 2010. Heat shock factor 1 ameliorates proteotoxicity in cooperation with the transcription factor NFAT. EMBO J **29:**3459–3469. http://dx.doi.org/10.1038/emboj.2010.225.
21. **Sullivan EK, Weirich CS, Guyon JR, Sif S, Kingston RE.** 2001. Transcriptional activation domains of human heat shock factor 1 recruit human SWI/SNF. Mol Cell Biol **21:**5826–5837. http://dx.doi.org/10.1128/MCB.21.17.5826-5837.2001.
22. **Xu D, Zalmas LP, La Thangue NB.** 2008. A transcription cofactor required for the heat-shock response. EMBO Rep **9:**662–669. http://dx.doi.org/10.1038/embor.2008.70.
23. **Altarejos JY, Montminy M.** 2011. CREB and the CRTC co-activators: sensors for hormonal and metabolic signals. Nat Rev Mol Cell Biol **12:**141–151. http://dx.doi.org/10.1038/nrm3072.
24. **Fujimoto M, Hayashida N, Katoh T, Oshima K, Shinkawa T, Prakasama R, Tan K, Inouye S, Takii R, Nakai A.** 2010. A novel mouse HSF3 has the potential to activate nonclassical heat-shock genes during heat shock. Mol Biol Cell **21:**106–116. http://dx.doi.org/10.1091/mbc.E09-07-0639.
25. **Inouye S, Fujimoto M, Nakamura T, Takaki E, Hayashida N, Hai T, Nakai A.** 2007. Heat shock transcription factor 1 opens chromatin structure of interleukin-6 promoter to facilitate binding of an activator or a repressor. J Biol Chem **282:**33210–33327. http://dx.doi.org/10.1074/jbc.M704471200.
26. **Langmead B, Trapnell C, Pop M, Salzberg SL.** 2009. Ultrafast and memory-efficient alignment of short DNA sequences to the human genome. Genome Biol **10:**R25. http://dx.doi.org/10.1186/gb-2009-10-3-r25.
27. **Nakato R, Itoh T, Shirahige K.** 2013. DROMPA: easy-to-handle peak calling and visualization software for the computational analysis and validation of ChIP-seq data. Genes Cells **18:**589–601. http://dx.doi.org/10.1111/gtc.12058.
28. **Kouzarides T.** 2007. Chromatin modifications and their function. Cell **128:**693–705. http://dx.doi.org/10.1016/j.cell.2007.02.005.
29. **Clapier CR, Cairns BR.** 2009. The biology of chromatin remodeling complexes. Annu Rev Biochem **78:**273–304. http://dx.doi.org/10.1146/annurev.biochem.77.062706.153223.
30. **Corey LL, Weirich CS, Benjamin IJ, Kingston RE.** 2003. Localized recruitment of a chromatin-remodeling activity by an activator in vivo drives transcriptional elongation. Genes Dev **17:**1392–1401. http://dx.doi.org/10.1101/gad.1071803.
31. **Shanware NP, Zhan L, Hutchinson JA, Kim SH, Williams LM, Tibbetts RS.** 2010. Conserved and distinct modes of CREB/ATF transcription factor regulation by PP2A/B56gamma and genotoxic stress. PLoS One **5**(8):e12173. http://dx.doi.org/10.1371/journal.pone.0012173.
32. **Walton KM, Rehfuss RP, Chrivia JC, Lochner JE, Goodman RH.** 1992. A dominant repressor of cyclic adenosine 3′,5′-monophosphate (cAMP)-regulated enhancer-binding protein activity inhibits the cAMP-mediated induction of the somatostatin promoter in vivo. Mol Endocrinol **6:**647–655. http://dx.doi.org/10.1210/mend.6.4.1350057.
33. **Kasper LH, Thomas MC, Zambetti GP, Brindle PK.** 2011. Double null cells reveal that CBP and p300 are dispensable for p53 targets p21 and Mdm2 but variably required for target genes of other signaling pathways. Cell Cycle **10:**212–221. http://dx.doi.org/10.4161/cc.10.2.14542.
34. **Westerheide SD, Anckar J, Stevens SM, Jr, Sistonen L, Morimoto RI.** 2009. Stress-inducible regulation of heat shock factor 1 by the deacetylase SIRT1. Science **323:**1063–1066. http://dx.doi.org/10.1126/science.1165946.
35. **Mendillo ML, Santagata S, Koeva M, Bell GW, Hu R, Tamimi RM, Fraenkel E, Ince TA, Whitesell L, Lindquist S.** 2012. HSF1 drives a transcriptional program distinct from heat shock to support highly malignant human cancers. Cell **150:**549–562. http://dx.doi.org/10.1016/j.cell.2012.06.031.
36. **Vihervaara A, Sergelius C, Vasara J, Blom MA, Elsing AN, Roos-Mattjus P, Sistonen L.** 2013. Transcriptional response to stress in the dynamic chromatin environment of cycling and mitotic cells. Proc Natl Acad Sci U S A **110:**E3388–3397. http://dx.doi.org/10.1073/pnas.1305275110.
37. **Kasper LH, Lerach S, Wang J, Wu S, Jeevan T, Brindle PK.** 2010. CBP/p300 double null cells reveal effect of coactivator level and diversity on CREB transactivation. EMBO J **29:**3660–3672. http://dx.doi.org/10.1038/emboj.2010.235.
38. **Wang Z, Zang C, Cui K, Schones DE, Barski A, Peng W, Zhao K.** 2009. Genome-wide mapping of HATs and HDACs reveals distinct functions in active and inactive genes. Cell **138:**1019–1031. http://dx.doi.org/10.1016/j.cell.2009.06.049.
39. **Li Q, Herrler M, Landsberger N, Kaludov N, Ogryzko VV, Nakatani Y, Wolffe AP.** 1998. Xenopus NF-Y pre-sets chromatin to potentiate p300 and acetylation-responsive transcription from the Xenopus hsp70 promoter in vivo. EMBO J **17:**6300–6315. http://dx.doi.org/10.1093/emboj/17.21.6300.
40. **Ghosh SK, Missra A, Gilmour DS.** 2011. Negative elongation factor accelerates the rate at which heat shock genes are shut off by facilitating dissociation of heat shock factor. Mol Cell Biol **31:**4232–4243. http://dx.doi.org/10.1128/MCB.05930-11.
41. **Raychaudhuri S, Loew C, Körner R, Pinkert S, Theis M, Hayer-Hartl M, Buchholz F, Hartl FU.** 2014. Interplay of acetyltransferase EP300 and the proteasome system in regulating heat shock transcription factor 1. Cell **156:**975–985. http://dx.doi.org/10.1016/j.cell.2014.01.055.
42. **Qiang L, Lin HV, Kim-Muller JY, Welch CL, Gu W, Accili D.** 2011. Proatherogenic abnormalities of lipid metabolism in SirT1 transgenic mice are mediated through Creb deacetylation. Cell Metab **14:**758–767. http://dx.doi.org/10.1016/j.cmet.2011.10.007.
43. **Mantamadiotis T, Lemberger T, Bleckmann SC, Kern H, Kretz O, Martin VA, Tronche F, Kellendonk C, Gau D, Kapfhammer J, Otto C, Schmid W, Schütz G.** 2002. Disruption of CREB function in brain leads to neurodegeneration. Nat Genet **31:**47–54. http://dx.doi.org/10.1038/ng882.
44. **Iijima-Ando K, Wu P, Drier EA, Iijima K, Yin JC.** 2005. cAMP-response element-binding protein and heat-shock protein 70 additively suppress polyglutamine-mediated toxicity in Drosophila. Proc Natl Acad Sci U S A **102:**10261–10266. http://dx.doi.org/10.1073/pnas.0503937102.
45. **Bleckmann SC, Blendy JA, Rudolph D, Monaghan AP, Schmid W, Schütz G.** 2002. Activating transcription factor 1 and CREB are important for cell survival during early mouse development. Mol Cell Biol **22:**1919–1925. http://dx.doi.org/10.1128/MCB.22.6.1919-1925.2002.